# Methyl-L-$^{11}$C-Methionine PET as a Diagnostic Marker for Malignant Progression in Patients with Glioma

Roland T. Ullrich*[1,2], Lutz Kracht*[1], Anna Brunn[3], Karl Herholz[4], Peter Frommolt[5], Hrvoje Miletic[6,7], Martina Deckert[3], Wolf-Dieter Heiss[1], and Andreas H. Jacobs[1,2,8,9]

[1]Max Planck Institute for Neurological Research with Klaus Joachim Zülch Laboratories, Cologne, Germany; [2]Center for Molecular Medicine, University of Cologne, Cologne, Germany; [3]Department of Neuropathology, University of Cologne, Cologne, Germany; [4]University of Manchester, Manchester, United Kingdom; [5]Institute of Medical Statistics, Informatics and Epidemiology, University of Cologne, Cologne, Germany; [6]Department of Biomedicine, University of Bergen, Bergen, Norway; [7]Department of Pathology, Haukeland University Hospital, Bergen, Norway; [8]Klinikum Fulda, Fulda, Germany; and [9]European Institute of Molecular Imaging–EIMI, University of Muenster, Muenster, Germany

Methyl-L-$^{11}$C-methionine ($^{11}$C-MET) PET has been shown to detect brain tumors with a high sensitivity and specificity. In this study, we investigated the potential of $^{11}$C-MET PET to noninvasively detect tumor progression in patients with gliomas. Moreover, we analyzed the relationship between changes in $^{11}$C-MET uptake on PET and changes in various molecular immunohistochemical markers during progression of gliomas. **Methods:** Twenty-four patients with histologically proven glioma were investigated repeatedly with $^{11}$C-MET PET. $^{11}$C-MET uptake was determined for a circular region of interest. Histologic and molecular analyses for tumor progression were performed after open surgery and stereotactic biopsy, respectively. **Results:** In patients with malignant progression, the mean increase in $^{11}$C-MET uptake was 54.4% (SD, 45.5%; range, 3.1%−162.2%), whereas in patients without a change in tumor grade, mean $^{11}$C-MET uptake did not significantly change (3.9%; SD, 13.7%; range, −24.4% to 26.3%). The difference in the change in $^{11}$C-MET uptake between the group with malignant progression and the group without malignant progression was highly significant ($P < 0.001$). Receiver-operating-curve analysis revealed a sensitivity of 90% and a specificity of 92.3% for the detection of malignant transformation by an increase in $^{11}$C-MET uptake of more than 14.6%. Increased $^{11}$C-MET uptake of more than 14.6% was indicative of malignant progression in all but 3 leave-one-out iterations. A detailed immunohistochemical analysis demonstrated a significant correlation between changes in $^{11}$C-MET uptake and the expression of vascular endothelial growth factor. **Conclusion:** These data suggest that $^{11}$C-MET-PET represents a noninvasive method to detect malignant progression in patients with gliomas. Moreover, the increase in $^{11}$C-MET uptake during malignant progression is reflected by an increase in angiogenesis-promoting markers as vascular endothelial growth factor.

**G**liomas are the most common primary brain tumors. More than 50% of gliomas belong to the malignant subtype glioblastoma (*1*). The most important criterion for therapeutic management and prognosis is histologic grading. WHO grade II gliomas have a median overall survival of more than 5 y, whereas anaplastic gliomas show a median survival of only 2–5 y (*2*). Most patients with glioblastoma succumb to the disease within 2 y (*2*). Thus, noninvasive imaging–based technology for the detection of malignant progression is required to select the best possible treatment regimen.

Several studies evaluated methyl-L-$^{11}$C-methionine ($^{11}$C-MET) PET for monitoring the effect of treatment and for differentiating recurrent tumor from radiation necrosis (*3–7*). Uptake of $^{11}$C-MET is facilitated by amino acid transporter, which is upregulated in glioma capillaries (*8*). $^{11}$C-MET PET detects the most malignant parts of brain tumors, as well as infiltrating areas, with high sensitivity and specificity (*9,10*). $^{11}$C-MET uptake correlates with microvessel density (*9*) and with the proliferative cell nuclear antigen index (*11*), demonstrating its relevance for evaluation of tumor malignancy. Although $^{11}$C-MET uptake correlates with tumor grade (*12,13*), high interindividual variability in $^{11}$C-MET uptake does not allow for accurate noninvasive grading (*14*).

The purpose of this study was to investigate the accuracy of intraindividual changes in $^{11}$C-MET uptake as a noninvasive indicator of malignant progression in gliomas and to compare changes in $^{11}$C-MET uptake with changes in the

molecular profile as determined by immunohistochemistry from tissue samples.

## MATERIALS AND METHODS

### Patients

This retrospective study included 24 patients with primary supratentorial cerebral gliomas (Table 1). We investigated 14 male patients and 10 female patients (mean age, 40 y; SD, 11.6 y). Each patient gave written informed consent for additional PET imaging, which is not a standard diagnostic tool for patients with gliomas in Germany. All patients who underwent repeated ^{11}C-MET PET and had a corresponding neuropathologic diagnosis during the period from 1993 to 2006 were included in the study (Fig. 1). The ^{11}C-MET PET investigations were part of the routine preoperative diagnostic procedure and were used to guide the biopsy so that the tumor portion with the highest ^{11}C-MET uptake would be obtained. Repeated PET investigations with corresponding biopsy were performed when there were findings suggestive of tumor progression on MRI or CT or suggestive clinical symptoms. The interval between PET measurements varied from 1 mo to 6 y. In total, data from 57 PET scans that had a corresponding histologic diagnosis within the following 3 weeks were available for 24 patients. ^{11}C-MET PET was performed after combined radio- and chemotherapy in 9 of 57 cases, after radiotherapy alone in 8 of 57 cases, and without preceding radio- or chemotherapy in 40 of 57 cases.

All 24 patients underwent baseline ^{11}C-MET PET, 16 of 24 underwent follow-up ^{11}C-MET once, 7 of 24 underwent follow-up ^{11}C-MET twice, and 1 of 24 underwent follow-up ^{11}C-MET 3 times. Information on the patients included age, sex, presence of contrast enhancement on MRI or CT, and extent of surgical resection (13 stereotactic biopsies, 23 subtotal resections, and 21 macroscopic total resections). The tumors were graded according to the World Health Organization (WHO) classification for neuroepithelial tumors (2).

In the initial histologic diagnosis, tumor types were distributed as follows: WHO grade II astrocytoma (n = 10), WHO grade III anaplastic astrocytoma (n = 3), WHO grade II oligoastrocytoma (n = 7), WHO grade III anaplastic oligoastrocytoma (n = 2), WHO grade II oligodendroglioma (n = 1), and WHO grade III anaplastic oligodendroglioma (n = 1) (Table 1).

### PET Studies

For PET imaging, we used an ECAT EXACT scanner (CTI/Siemens; in-plane full width at half maximum, 6 mm; slice thickness, 3.375 mm; axial field of view, 162 mm) and an ECAT EXACT HR scanner (CTI/Siemens; in-plane full width at half maximum, 3.6 mm; slice thickness, 3.125 mm; axial field of view, 150 mm) (15,16). Subsequent imaging was performed on the same scanner. All patients fasted for at least 4 h before undergoing PET. Images were acquired with the patient supine with eyes closed. Before tracer application, a 10-min transmission scan with 3 rotating $^{68}$Ga/$^{68}$Ge sources was obtained. ^{11}C-MET was synthesized according the method of Berger et al. (17) and injected intravenously as a bolus injection of 740 MBq (20 mCi). Accumulation of the tracer was recorded 0–60 min after tracer injection. For assessment of ^{11}C-MET PET images, frames recorded 20–60 min after tracer application in 47 transaxial slices of the entire brain were used. The spatial resolution was 6 mm or better in all dimensions.

**TABLE 1.** Patient Data at Study Entry

| Patient no. | Age (y) | Sex | Initial histology and WHO grade | Resection | Radiotherapy before PET | Chemotherapy before PET |
|---|---|---|---|---|---|---|
| 1 | 32 | F | Astrocytoma II | T/P | Yes (9)/yes (3) | Yes (9)/no |
| 2 | 46 | F | Oligoastrocytoma II | S/P | No/no | No/no |
| 3 | 10 | M | Astrocytoma II | T/T | No/yes (6) | No/yes (6) |
| 4 | 40 | F | Astrocytoma II | P/P/P | No/no/yes (36) | No/no/yes (36) |
| 5 | 28 | M | Astrocytoma II | S/S | No/yes (150) | No/no |
| 6 | 49 | F | Oligoastrocytoma II | T/T | No/no | No/no |
| 7 | 26 | M | Oligoastrocytoma II | T/P/P | No/no/yes (159) | No/no/no |
| 8 | 35 | M | Astrocytoma III | S/S | No/yes (24) | No/yes (24) |
| 9 | 32 | F | Oligoastrocytoma II | T/T/T/T | No/yes (376)/yes (53)/no | No/no/no/no |
| 10 | 35 | F | Oligoastrocytoma II | P/P | Yes (156)/no | No/no |
| 11 | 53 | M | Oligodendroglioma II | T/P/P | No/yes (126)/no | No/no/no |
| 12 | 29 | M | Astrocytoma II | T/S | No/no | No/no |
| 13 | 40 | M | Oligoastrocytoma II | T/T/P | No/no/yes (12) | No/no/yes (12) |
| 14 | 30 | M | Oligoastrocytoma III | P/P | No/no | No/no |
| 15 | 23 | M | Astrocytoma III | P/T | No/yes (50) | No/yes (50) |
| 16 | 27 | F | Oligodendroglioma III | S/P | No/yes (9) | No/yes (9) |
| 17 | 39 | M | Oligoastrocytoma II | T/T | No/no | No/no |
| 18 | 38 | F | Astrocytoma II | T/T/S | No/no/yes (102) | No/no/no |
| 19 | 57 | F | Astrocytoma II | S/T | No/no | No/no |
| 20 | 37 | M | Astrocytoma II | S/T/T | No/no/yes (25) | No/no/yes (25) |
| 21 | 34 | M | Astrocytoma II | P/S | No/no | No/no |
| 22 | 59 | F | Astrocytoma II | P/P/P | No/no/no | No/no/no |
| 23 | 47 | M | Oligoastrocytoma III | O/P | No/yes (25) | No/yes (25) |
| 24 | 58 | M | Astrocytoma III | S/P | No/no | No/no |

T = total resection; P = partial resection; S = stereotactic biopsy; O = open biopsy.
Data in parentheses are interval (in weeks) between PET scan and chemo- or radiotherapy.

**FIGURE 1.** ^{11}C-MET PET of 39-y-old man with malignant progression of recurrent glioma. (A) Newly diagnosed grade II astrocytoma with average ^{11}C-MET uptake of 1.3 to contralateral gray matter, with no enhancement on contrast-enhanced CT and no immunohistochemical VEGF expression. (B) One year later, patient presented with malignant progression to grade III astrocytoma associated with significant increase in ^{11}C-MET uptake (to 2.1-fold) and only slight contrast enhancement outside metabolically active tumor. Histologic analysis from resection showed increase in cellularity, numerous pleomorphic nuclei, and low VEGF expression. (C) In following year, resection of tumor again confirmed malignant progression to glioblastoma multiforme, showing markedly increased uptake of ^{11}C-MET (to 2.8-fold), marginal contrast enhancement on MRI, and ~35% of tumor cells expressing VEGF (original magnification, ×400). PET-guided biopsies were taken from region with highest ^{11}C-MET uptake, which was in different locations within same tumor over time.
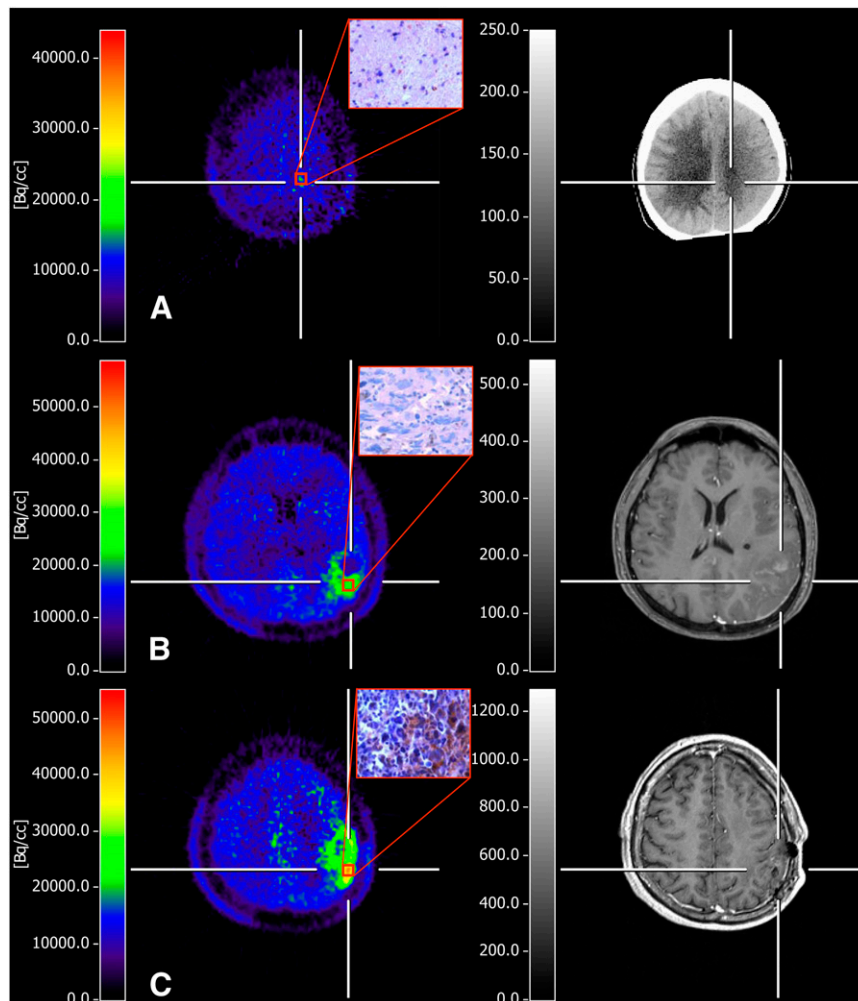
In 20 of 24 patients, 48 of 57 PET scans had corresponding contrast-enhanced MRI ($n = 36$) or CT ($n = 12$) scans. In 12 of 24 patients, MRI and PET were performed, in 6 of 24 patients MRI and CT and PET were performed, in 2 of 24 patients CT and PET were performed, and in 4 of 24 patients only PET was performed. Regions of ^{11}C-MET uptake were compared with areas of contrast enhancement on MRI or CT.

PET data were evaluated using a region-of-interest analysis. Because ^{11}C-MET uptake at later imaging times more specifically reflects transport activity, we used summed images covering the time frame 20–60 min after injection for data analysis. As described by Herholz et al., a circular region of interest 7 mm in diameter was placed on the area of highest ^{11}C-MET uptake to determine the maximal tracer uptake (*18*). A mirrored, contralateral region of interest of the same diameter was placed as a reference. The relative index of ^{11}C-MET uptake was calculated as the ratio of tumor area to reference area. The change in ^{11}C-MET uptake was defined as the relative percentage change in ^{11}C-MET uptake between 2 subsequent scans of the same patient.

### MRI/CT Studies

MRI was performed on a 1.5-T system (Gyroscan ACS-NT; Philips Medical Systems) using a head coil. T1-weighted spin-echo enhanced images were acquired with a slice thickness of 2 mm and a matrix of 512 × 512 pixels. To monitor gadopentetate dimeglumine enhancement of the tumors, we used a T1-weighted 3-dimensional gradient-echo sequence. CT was performed after administration of contrast medium (Solutrast 300R; Bracco). We acquired 22–40 CT images 2 mm thick.

### Histologic Analysis

Histologic analysis and immunohistochemistry of the biopsy samples of the initial tumors of all patients, as well as recurrences obtained by stereotactic biopsy or open surgery, were performed on formalin-fixed, paraffin-embedded 4-μm sections. For immunohistochemistry, we applied an automated staining system (BioGenex) using the avidin-biotin-peroxidase complex technique, with 3,3′-diaminobenzidine as chromogene and $H_2O_2$ as cosubstrate. In brief, classification of the tumors according to the WHO classification of neuroepithelial tumors was based on hematoxylin and eosin staining and immunohistochemistry with monoclonal antibodies against rabbit antihuman MIB-1 (DCS, Innovative Diagnostik-Systeme; clone SP6; dilution, 1:200) and mouse antihuman p53 protein (BioGenex; clone 1801; dilution, 1:200) and polyclonal rabbit antihuman antibodies against glial fibrillary acidic protein and S100 protein (Dako; dilution, glial fibrillary acidic protein, 1:1,000; S100-protein, 1:2,000). Advanced immunohistochemistry was performed with the following monoclonal mouse antihuman antibodies: epidermal growth factor receptor (Merck; clone E30; dilution, 1:20), platelet-derived growth factor

receptor (BD Biosciences; clone 28; dilution, 1:200), retinoblastoma protein (pRb) (Zymed Laboratories; clone Rb1; dilution, 1:50), pentaerythritol tetranitrate (PTEN) (Biogenex; clone 28H6; dilution, 1:10), and vascular endothelial growth factor (VEGF) (DCS; clone VG1; dilution, 1:50). Histologic evaluation was performed by 2 independent neuropathologists. The number of immunoreactive nuclei was determined, comprising 3 areas (F1, F2, and F3) of 3 high-power fields each, with maximal frequency, moderate frequency, and minimal frequency, respectively, of immunoreactive nuclei. The number of positive nuclei was determined as F1 plus F2 plus F3, divided by 3 (%).

### Statistical Analysis

Statistical analyses were performed using SPSS software (release 11.0.1, SPSS Inc.). For correlation analysis, the Pearson method was applied, with subsequent parametric tests; 2-sample ANOVA was used for comparisons between the groups with and without malignant progression. Tests were performed 2-sided at a significance level of 0.05, and the $P$ values were understood in an explorative sense regarding the multiple-hypothesis problem. The sensitivity and specificity of changes in $^{11}$C-MET uptake were calculated for several thresholds, and the optimum cut-off was determined by receiver-operating-characteristic analysis. An iterative leave-one-out approach was used to validate the receiver-operating-characteristic analysis. At each step, 1 case (i.e. 1 follow-up) was left out of the analysis; a fit of the model was produced for the remaining follow-ups, and a malignant progression prediction was made for the left-out case. Thus, each follow-up value was compared with the cohort of the remaining 32 of 33 values with regard to its individual percentage change in $^{11}$C-MET uptake. Moreover, baseline $^{11}$C-MET uptake was included as a covariate in a Cox regression model to investigate its relation to the time to histologic progression. To avoid an artificial reduction of variance caused by the mixing of independent and dependent observations, we used the data of only the first follow-up investigation ($n = 24$) for all methods of statistical inference (Pearson method and 2-sample ANOVA).

### RESULTS

#### Malignant Progression as Detected by $^{11}$C-MET PET

For evaluation of the correlation between $^{11}$C-MET uptake and histologic progression of the tumor, we calculated the percentage change in $^{11}$C-MET uptake between the prior $^{11}$C-MET PET examination and the subsequent examination. The percentage change in $^{11}$C-MET uptake was then compared with the progression as assessed by histology and immunohistochemistry.

For the 24 patients, 57 PET scans with corresponding histologic investigations were available. Among the 24 patients, 16 patients underwent 1 follow-up investigation, 7 patients underwent 2, and 1 patient underwent 3, leading to a total of 33 follow-up investigations. Among these 33, 20 showed histologically proven malignant progression of the tumor. Eleven tumors progressed from grade II to grade III, 6 from grade III to grade IV, and 3 from grade II to grade IV. In 13 cases, the biopsy did not indicate malignant progression.

The mean percentage increase in $^{11}$C-MET uptake between PET studies in the group with histologically proven malignant progression was 54.4% (SD, 45.5%;

range, 3.1%−162.2%). In contrast, the mean percentage change in $^{11}$C-MET uptake in the group without a change in tumor grade was 3.9% (SD, 13.7%; range, −24.4% to 26.3%) (Fig. 2). The mean difference in change in $^{11}$C-MET uptake between the group with malignant progression and the group without was highly significant ($P < 0.001$).

To identify the percentage increase in $^{11}$C-MET uptake that best distinguished malignant from nonmalignant progression, we performed a receiver-operating-characteristic analysis (Fig. 3) and calculated the sensitivity and specificity for each value. The percentage change in $^{11}$C-MET uptake that best determined malignant progression was 14.6% (sensitivity, 90%; specificity, 92.3%). The area under the curve was 0.96. At a threshold of 14.6%, we identified in only 2 of 20 cases (10%) false-negative $^{11}$C-MET uptake findings of malignant progression. In both these tumors, the percentage increase in $^{11}$C-MET uptake was less than 14.6% (3.1% and 9.0%, respectively). Malignant progression in both these cases was from grade III to grade IV. We had only 1 false-positive $^{11}$C-MET uptake finding; uptake increased by 26.3% whereas the tumor remained histologically stable at grade II. For the 14.6% threshold, positive predictive value was 94.7% and negative predictive value was 85.7%. In the 33-fold cross-validation using the leave-one-out strategy, we correctly classified 30 of 33 follow-up investigations; 1 observation was false-positive and 2 were false-negative, using the 14.6% threshold for change in $^{11}$C-MET uptake.

The increase in $^{11}$C-MET uptake clearly differed between progression from grade II to grade III and progression from grade III to grade IV, being 72.9% (SD, 46.2%) and 33.5% (SD, 35.4%), respectively (Table 2). The change in uptake for progression from grade II to IV was heterogeneous: 77% in 1 case but only 18.5% and 18.9% in the other 2 cases.

We further analyzed the influence of baseline $^{11}$C-MET uptake on the time to tumor progression but found no interrelationship between these parameters ($P = 0.96$).
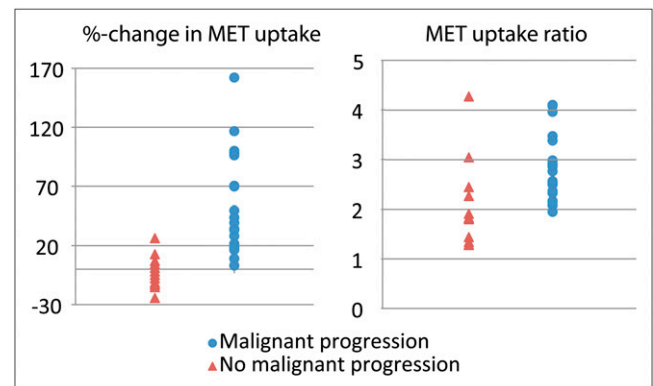


**FIGURE 2.** Comparison of value of $^{11}$C-MET uptake ratio at time of biopsy vs. percentage change in $^{11}$C-MET uptake in distinguishing malignant from nonmalignant progression.
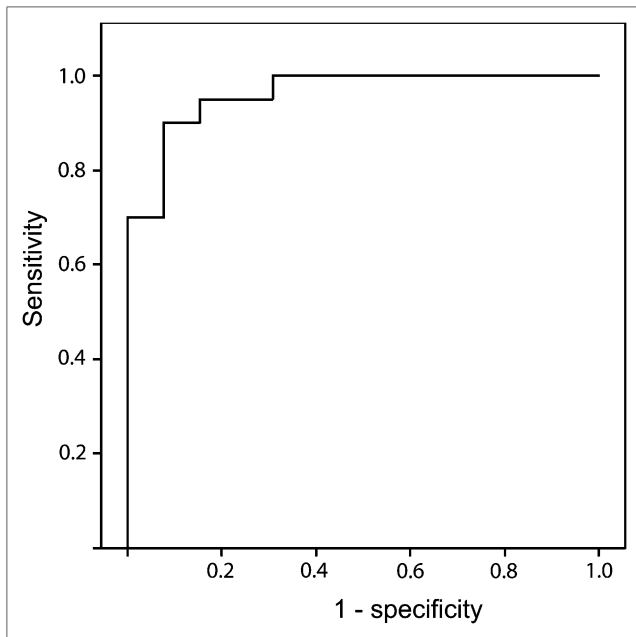
**FIGURE 3.** Receiver operating characteristic analysis to identify change in ^{11}C-MET uptake for differentiation between malignant progression of tumor grade and no malignant progression. Percentage increase that best distinguished malignant progression from no malignant progression was at threshold of 14.6%, with sensitivity of 90% and specificity of 92.3%.

Moreover, we compared absolute ^{11}C-MET uptake ratios at follow-up with changes in ^{11}C-MET uptake for their potential in distinguishing between malignant and non-malignant progression: for changes in ^{11}C-MET uptake in patients with malignant progression (38.2%−83.3%) and without malignant progression (−13.2% to 6.6%), the 95% confidence intervals were separated, whereas for absolute ^{11}C-MET uptake ratios at follow-up, the 95% confidence intervals overlapped (1.5–2.7 uptake ratio for malignant progression and 2.4–3.1 uptake ratio for stable disease), suggesting that relative changes between uptake ratios more sensitively distinguish malignant progression from stable disease (Fig. 2).

### Changes in Contrast Enhancement on MRI or CT During Malignant Progression

For 48 of 57 PET investigations, corresponding MRI ($n = 36$) or CT ($n = 12$) had been performed within 6 d beforehand. Using a yes/no categorization, we analyzed for the presence or absence of changes in tumor accumulation

of contrast agent in 28 PET-corresponding follow-up investigations. We compared regions of contrast enhancement on the MRI or CT with regions of increased ^{11}C-MET uptake (Table 3).

The MRI or CT measurements were obtained in 17 cases of histologically proven malignant progression and in 11 cases of no progression. We did not observe coherence between newly appearing contrast enhancement on MRI and an increase in ^{11}C-MET uptake and histologic malignant progression. In 8 of 17 cases with histologically proven malignant progression, tumor progression could be detected by newly appearing contrast enhancement on MRI or CT. In 6 of 17 cases, we observed contrast enhancement at baseline as well as at follow-up. In 3 of 17 cases, we observed contrast enhancement neither at baseline nor at follow-up.

In 7 of 11 cases without histologically proven malignant progression, we observed contrast enhancement on baseline MRI or CT as well as at follow-up. In 1 of 11 cases, MRI and CT showed contrast enhancement neither in the prior investigation nor in the subsequent investigation. Three of 11 patients showed newly appearing contrast enhancement on MRI without histologic signs of malignant progression.

### Correlation of Molecular Changes on Immunostaining with Metabolic Changes on ^{11}C-MET PET

Histologic analysis was performed on the 52 biopsy samples that corresponded to the PET investigation. All 52 samples were immunostained for Ki-67, VEGF, epidermal growth factor receptor, p53, PTEN, platelet-derived growth factor receptor, and pRb. To avoid an artificial reduction of variance caused by mixing independent and dependent observations, we used only the data of the first follow-up investigations in determining correlations between changes in ^{11}C-MET uptake and changes in the expression of molecular markers. Changes in the expression level of VEGF correlated to changes in ^{11}C-MET uptake ($r = 0.62$, $P = 0.005$), indicating that an increase in ^{11}C-MET uptake was related to tumor angiogenesis (Fig. 4). No significant correlation was observed between changes in ^{11}C-MET uptake and changes in the expression pattern of Ki-67, epidermal growth factor receptor, p53, PTEN, platelet-derived growth factor receptor, or pRb.

### DISCUSSION

This study indicated that ^{11}C-MET PET enables the noninvasive detection of malignant progression in patients who have gliomas with clinical or radiologic findings of

**TABLE 2.** Changes in ^{11}C-MET Uptake in Patients Without Tumor Progression or with Various Degrees of Progression

| Parameter | Malignant progression | | | |
| --- | --- | --- | --- | --- |
| | None ($n = 13$) | From grade II to III ($n = 11$) | From grade III to IV ($n = 6$) | From grade II to IV ($n = 3$) |
| Mean | 3.9% | 72.9% | 33.5% | 38.1% |
| SD | 13.7% | 46.2% | 35.4% | 33.6% |

**TABLE 3.** Changes in Contrast Enhancement in Relation to Histologically Proven Malignant Progression

| Malignant progression | Newly appearing contrast enhancement on MRI/CT | |
|---|---|---|
| | Present | Absent |
| Present | 8 | 9 |
| Absent | 3 | 8 |

tumor progression. Moreover, a correlation was found between changes in ^{11}C-MET uptake and changes in VEGF expression, suggesting a potential link between amino acid transport and tumor angiogenesis.

In gliomas, the early detection of malignant transformation from WHO grade II to grade III or from WHO grade III to grade IV is of high clinical importance because the decision to apply a specific treatment depends mainly on the WHO grade. The mean interval for progression from low-grade glioma to high-grade glioma ranges from 4 to 5 y (19,20). Moreover, malignant progression in gliomas is unpredictable and in many cases not clearly detectable on the basis of clinical symptoms or MRI findings alone. Thus, ^{11}C-MET PET might provide sensitive and specific information on tumor activity and malignant progression in patients with gliomas when a clear answer cannot be obtained on the basis of clinical or MRI findings alone. Repeated ^{11}C-MET PET gives a clear indication of malignant glioma progression and should be used in conjunction with MRI to decrease the need for diagnostic stereotactic interventions.

One major limitation of the study was the lack of an independent sample of patients without clinical or radiologic signs of malignant progression to validate the accuracy of the calculated threshold for the change in ^{11}C-MET uptake. However, because of the radiation exposure and the risks related to invasive stereotactic biopsies, the inclusion of patients without signs suggestive of malignant pro-
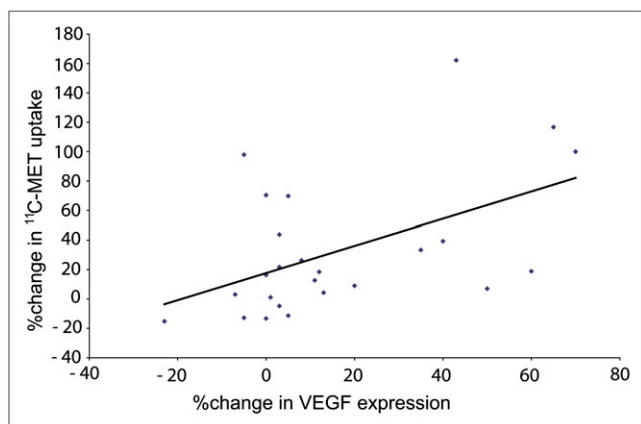


**FIGURE 4.** Correlation between changes in expression of VEGF and changes in ^{11}C-MET uptake during first follow-up investigation.

gression is not ethically feasible. Thus, we performed a cross-validation in a leave-one-out strategy for all receiver-operating-characteristic analyses to confirm whether the assessed threshold for changes in ^{11}C-MET uptake was accurate in indicating malignant progression. However, 1 patient in the study showed an increase in ^{11}C-MET uptake without histologic signs of malignant progression. Thus, future prospective studies with constant time points between ^{11}C-MET PET investigations are required to confirm the accuracy of the determined threshold and to validate the specificity of ^{11}C-MET PET in detecting malignant progression.

Although it has been shown that the high interindividual variability of ^{11}C-MET PET does not allow for glioma grading at first diagnosis (14)—most likely because of the differential effects of oligodendroglial tumor components on tumor vessels and the related amino acid uptake—we here demonstrated that ^{11}C-MET PET may be valuable for the intraindividual follow-up of biologically active glioma tissue after treatment to determine the time of tumor progression. The important parameter is not the absolute ^{11}C-MET uptake ratio but the change between two ^{11}C-MET measurements within the same individual.

We further sought to analyze the relationship between changes in ^{11}C-MET uptake and molecular markers as assessed by immunohistochemistry. We found that changes in ^{11}C-MET uptake are related to VEGF expression. It is well known that the mammalian target of rapamycin is downstream from the VEGF/VEGF receptor 2 pathway via phosphatidylinositol-3′-kinase/AKT regulated by VEGF (21,22). Mammalian target of rapamycin again modulates amino acid transport by regulating the expression of L-type amino acid transporter 1 (23). Although the correlation between changes in ^{11}C-MET uptake and VEGF expression is relatively weak, we hypothesize that there might be a crosslink between VEGF receptor 2 signaling and amino acid transport. The activation of VEGF/VEGF receptor 2 signaling induces mammalian target of rapamycin kinase activity, with mammalian target of rapamycin being a key enzyme regulating amino acid transport. The hypothesis that ^{11}C-MET uptake may serve as a surrogate marker for activated VEGF receptor signaling remains to be investigated. We did not find a significant correlation between changes in epidermal growth factor receptor, PTEN, pRb, p53, Ki-67, or platelet-derived growth factor receptor expression and changes in ^{11}C-MET uptake. Although epidermal growth factor, PTEN, pRb, p53, and Ki-67 are major factors in the genetic pathway to malignant transformation in gliomas, they contribute mainly to changes in the cell cycle and therefore cell proliferation (24–27).

One major effect of VEGF is the induction of vascular permeability, with consequent disruption of the vascular barrier (28,29). To evaluate the relationship between ^{11}C-MET uptake and leakage of the blood–brain barrier, we further analyzed whether ^{11}C-MET uptake is accompanied by contrast enhancement on MRI as a marker of high

vascular permeability. Interestingly, we observed in 21% of the patients ^{11}C-MET accumulation without contrast enhancement on MRI. This observation underlines—as reported in previous studies—the fact that ^{11}C-MET uptake is not related mainly to an elevated diffusion through leakage of endothelial cell–cell junctions but to specific amino acid transporter systems (8,18,30). Consequently, ^{11}C-MET can be considered a radiolabeled tracer for determining the activity of the amino acid transport system independently of the state of the blood–brain barrier.

We further examined the value of newly appearing contrast enhancement in detecting malignant progression. In this study, contrast enhancement on MRI or CT was not indicative of malignant progression in WHO grade. Although not all our patients underwent MRI, these findings are in line with a previous study by Scott at al. describing the inaccuracy of contrast enhancement as a marker for assessing glioma malignancy in 314 patients (31). Over the study period, new MRI parameters such as diffusion or perfusion-weighted imaging were implemented in the diagnosis of brain tumors. It remains to be investigated whether changes in diffusion or perfusion-weighted imaging might allow for the detection of malignant progression in patients with gliomas, as well.

## CONCLUSION

These data suggest that ^{11}C-MET PET is a marker for the noninvasive detection of malignant progression in patients with gliomas. Because of the relatively few patients in this retrospective study, prospective studies are required to further validate these results.

## REFERENCES

1. *Statistical Report: Primary Brain Tumors in the United States, 1997–2001.* Hinsdale, IL: Central Brain Tumor Registry of the United States; 2004.
2. Louis DN, Ohgaki H, Wiestler OD, et al. The 2007 WHO classification of tumours of the central nervous system. *Acta Neuropathol.* 2007;114:97–109.
3. Tsuyuguchi N, Takami T, Sunada I, et al. Methionine positron emission tomography for differentiation of recurrent brain tumor and radiation necrosis after stereotactic radiosurgery: in malignant glioma. *Ann Nucl Med.* 2004;18:291–296.
4. Jacobs AH, Kracht LW, Gossmann A, et al. Imaging in neurooncology. *NeuroRx.* 2005;2:333–347.
5. Jacobs AH, Li H, Winkeler A, et al. PET-based molecular imaging in neuroscience. *Eur J Nucl Med Mol Imaging.* 2003;30:1051–1065.
6. Thiel A, Pietrzyk U, Sturm V, Herholz K, Hovels M, Schroder R. Enhanced accuracy in differential diagnosis of radiation necrosis by positron emission tomography–magnetic resonance imaging coregistration: technical case report. *Neurosurgery.* 2000;46:232–234.
7. Van Laere K, Ceyssens S, Van Calenbergh F, et al. Direct comparison of ^{18}F-FDG and ^{11}C-methionine PET in suspected recurrence of glioma: sensitivity, inter-observer variability and prognostic value. *Eur J Nucl Med Mol Imaging.* 2005;32:39–51.
8. Miyagawa T, Oku T, Uehara H, et al. "Facilitated" amino acid transport is upregulated in brain tumors. *J Cereb Blood Flow Metab.* 1998;18:500–509.
9. Kracht LW, Friese M, Herholz K, et al. Methyl-[^{11}C]-l-methionine uptake as measured by positron emission tomography correlates to microvessel density in patients with glioma. *Eur J Nucl Med Mol Imaging.* 2003;30:868–873.
10. Kracht LW, Miletic H, Busch S, et al. Delineation of brain tumor extent with [^{11}C]L-methionine positron emission tomography: local comparison with stereotactic histopathology. *Clin Cancer Res.* 2004;10:7163–7170.
11. Sato N, Suzuki M, Kuwata N, et al. Evaluation of the malignancy of glioma using ^{11}C-methionine positron emission tomography and proliferating cell nuclear antigen staining. *Neurosurg Rev.* 1999;22:210–214.
12. Derlon JM, Bourdet C, Bustany P, et al. [^{11}C]L-methionine uptake in gliomas. *Neurosurgery.* 1989;25:720–728.
13. Ogawa T, Shishido F, Kanno I, et al. Cerebral glioma: evaluation with methionine PET. *Radiology.* 1993;186:45–53.
14. Ceyssens S, Van Laere K, de Groot T, Goffin J, Bormans G, Mortelmans L. [^{11}C]methionine PET, histopathology, and survival in primary brain tumors and recurrence. *Am J Neuroradiol.* 2006;27:1432–1437.
15. Wienhard K, Eriksson L, Grootoonk S, Casey M, Pietrzyk U, Heiss WD. Performance evaluation of the positron scanner ECAT EXACT. *J Comput Assist Tomogr.* 1992;16:804–813.
16. Wienhard K, Dahlbom M, Eriksson L, et al. The ECAT EXACT HR: performance of a new high resolution positron scanner. *J Comput Assist Tomogr.* 1994;18:110–118.
17. Berger G, Maziere M, Knipper R, Prenant C, Comar D. Automated synthesis of ^{11}C-labelled radiopharmaceuticals: imipramine, chlorpromazine, nicotine and methionine. *Int J Appl Radiat Isot.* 1979;30:393–399.
18. Herholz K, Holzer T, Bauer B, et al. ^{11}C-methionine PET for differential diagnosis of low-grade gliomas. *Neurology.* 1998;50:1316–1322.
19. Watanabe K, Sato K, Biernat W, et al. Incidence and timing of p53 mutations during astrocytoma progression in patients with multiple biopsies. *Clin Cancer Res.* 1997;3:523–530.
20. McCormack BM, Miller DC, Budzilovich GN, Voorhees GJ, Ransohoff J. Treatment and survival of low-grade astrocytoma in adults: 1977–1988. *Neurosurgery.* 1992;31:636–642.
21. Riesterer O, Zingg D, Hummerjohann J, Bodis S, Pruschy M. Degradation of PKB/Akt protein by inhibition of the VEGF receptor/mTOR pathway in endothelial cells. *Oncogene.* 2004;23:4624–4635.
22. Kim BW, Choi M, Kim YS, et al. Vascular endothelial growth factor (VEGF) signaling regulates hippocampal neurons by elevation of intracellular calcium and activation of calcium/calmodulin protein kinase II and mammalian target of rapamycin. *Cell Signal.* 2008;20:714–725.
23. Fuchs BC, Bode BP. Amino acid transporters ASCT2 and LAT1 in cancer: partners in crime? *Semin Cancer Biol.* 2005;15:254–266.
24. Narita Y, Nagane M, Mishima K, Huang HJ, Furnari FB, Cavenee WK. Mutant epidermal growth factor receptor signaling down-regulates p27 through activation of the phosphatidylinositol 3-kinase/Akt pathway in glioblastomas. *Cancer Res.* 2002;62:6764–6769.
25. Mellinghoff IK, Wang MY, Vivanco I, et al. Molecular determinants of the response of glioblastomas to EGFR kinase inhibitors. *N Engl J Med.* 2005;353:2012–2024.
26. Giacinti C, Giordano A. RB and cell cycle progression. *Oncogene.* 2006;25:5220–5227.
27. Ohgaki H, Dessen P, Jourde B, et al. Genetic pathways to glioblastoma: a population-based study. *Cancer Res.* 2004;64:6892–6899.
28. Weis SM, Cheresh DA. Pathophysiological consequences of VEGF-induced vascular permeability. *Nature.* 2005;437:497–504.
29. Rosenstein JM, Mani N, Silverman WF, Krum JM. Patterns of brain angiogenesis after vascular endothelial growth factor administration in vitro and in vivo. *Proc Natl Acad Sci USA.* 1998;95:7086–7091.
30. Jager PL, Vaalburg W, Pruim J, de Vries EG, Langen KJ, Piers DA. Radiolabeled amino acids: basic aspects and clinical applications in oncology. *J Nucl Med.* 2001;42:432–445.
31. Scott JN, Brasher PM, Sevick RJ, Rewcastle NB, Forsyth PA. How often are nonenhancing supratentorial gliomas malignant? A population study. *Neurology.* 2002;59:947–949.